Chin. J. Astron. Astrophys. Vol.0 (200x) No.0, 000–000
(*http://www.chjaa.org*)

Chinese Journal of Astronomy and Astrophysics

Are Seyfert 2 Galaxies without Polarized Broad Emission Lines More Obscured?

Xin-Wen Shu[1,2] ⋆, Jun-Xian Wang[1,2] and Peng Jiang[1,2]

[1] Center for Astrophysics, University of Science and Technology of China (USTC), Hefei, Anhui 230026, China

[2] Joint Institute for Galaxy and Cosmology, USTC and Shanghai Astronomical Observatory, Chinese Academy of Sciences, Hefei, Anhui 230026, China

Abstract The new $XMM-Newton$ data of seven Seyfert 2 galaxies with optical spectropolarimetric observations are presented. The analysis of 0.5 – 10 keV spectra shows that all four Seyfert 2 galaxies with polarized broad lines (PBLs) are absorbed with $N_{\rm H} < 10^{24}$ cm^{-2}, while two of three Seyfert 2 galaxies without PBLs have evidence suggesting Compton-thick obscuration, supporting the conclusion that Seyfert 2 galaxies without PBLs are more obscured than those with PBLs. Adding the measured obscuration indicators ($N_{\rm H}$, T ratio, and Fe Kα line EW) of six luminous AGNs to our previous sample improves the significance level of the difference in absorption from 92.3% to 96.3% for $N_{\rm H}$, 99.1% to 99.4% for T ratio, and 95.3% to 97.4% for Fe Kα line EW. The present results support and enhance the suggestions that the absence of PBLs in Seyfert 2 galaxies can be explained by larger viewing angle of line of sight to the putative dusty torus, which lead to the obscuration of broad-line scattering screen, as expected by the unification model.

Key words: galaxies: active — galaxies: individual (NGC 513, NGC 1144, NGC 6890, NGC 7682, MCG -3-58-7, F02581-1136, UGC 6100) — galaxies: Seyfert — X-rays: galaxies — polarization

1 INTRODUCTION

The Seyfert unification model postulates that Seyfert 1 and 2 galaxies (hereafter, Sy1s and Sy2s) are intrinsically the same and the existence of an optical thick region (the "torus") obscures the broad-line region (BLR) in Sy2s (Antonucci 1993). The orientation of this torus relative to our line of sight then determines whether the galaxy is classified as a Seyfert 1 or 2 galaxy. The most important observational evidence for this orientation-based unification model is the detection of polarized broad emission lines (hereafter PBLs) in Sy2s in optical spectropolarimetry (Antonucci & Miller 1985; Miller & Goodrich 1990; Young et al. 1996; Heisler et al. 1997; Moran et al. 2000; Lumsden et al. 2001, 2004; Tran 2001). Additional evidence for this simple unification model comes from X-ray studies which have demonstrated that many Sy2s show heavy absorption along the line of sight (Turner et al. 1997; Bassani et al. 1999). In the local universe, about half of Sy2s are found to be Compton-thick sources with $N_{\rm H} > 10^{24}$ cm $^{-2}$ (Risaliti et al. 1999; Cappi et al. 2006).

However, up to 50% Sy2s do not show PBLs in the spectropolarimetric observations (Tran 2001, 2003; Gu & Huang 2002). Several studies indicated that the presence or absence of PBLs depends on the AGN luminosity, with PBL sources having larger luminosities (Tran 2001; Lumsden & Alexander 2001). More specifically, Nicastro et al. (2003) suggested that the absence of PBLs corresponds to low values of accretion rate on to the central black hole. While Tran (2001) proposed the existence of a population of AGNs which

⋆ E-mail: xwshu@mail.ustc.edu.cn

are intrinsically weak and lack of BLRs, Lumsden et al. (2001) argued that the detectability of PBLs is mainly determined by the relative luminosity of the active core to the host galaxy (see also Alexander 2001; Gu et al. 2001).

Recently, by focusing on Sy2s with $L_{[O\ III]} > 10^{41}$ erg s^{-1}, Shu et al. (2007, hereafter Paper I) have shown that, in additional to the luminosity, the nuclear obscuration also plays a significant role in the visibility of PBL. In Paper I we found that Sy2s without PBLs (hereafter NPBL Sy2s) are more obscured in X-rays than Sy2s with PBLs (hereafter PBL Sy2s). This is in good agreement with the model proposed in Heisler et al. (1997), who suggested that the absence of PBLs could be attributed to edge-on line of sight and hidden of electron scattering region (see also Taniguchi & Anabuki 1999).

The sample discussed in Paper I includes 27 PBL Sy2s and 15 NPBL Sy2s with $L_{[O\ III]} > 10^{41}$ erg s^{-1} and X-ray observations available. In this paper we present new released $XMM-Newton$ 0.5 – 10 keV spectra of seven Sy2s with optical spectropolarimetric observations, six of which have $L_{[O\ III]} > 10^{41}$ erg s^{-1}. These new X-ray observations enlarge our sample of NPBL Sy2s from 15 to 17, and PBL Sy2s from 27 to 31, providing a chance to verify the results in Paper I. Section 2 details the $XMM-Newton$ observations and data analysis. X-ray spectra are analyzed in Section 3. Results are discussed in Section 4. Throughout this paper the cosmological parameters $H_0 = 70$ km s^{-1} Mpc^{-1}, $\Omega_m = 0.27$, and $\Omega_\lambda = 0.73$ are adopted.

2 OBSERVATIONS AND DATA ANALYSIS

The $XMM-Newton$ observations presented here have been performed between May 2005 and January 2006 with the EPIC PN (Strüder et al. 2001) detector and MOS (Turner et al. 2001) cameras operating in full-frame mode. In this paper, for simplicity only data from the EPIC PN camera will be discussed. Data have been processed using the Science Analysis Software (SAS version 6.5) and have been analyzed using standard software package (FTOOLS 5.0). The latest calibration files released by the EPIC team have been used. Details of the observations with redshift, coordinates (J2000.0), dates of the observations, PN net exposures, observation IDs, extinction-corrected [O III] λ5007 luminosities, and spectropolarimetric properties are reported in Table 1.

The event lists produced from the pipeline were filtered to ignore periods of high background flaring, by applying fixed thresholds on the single-event, E>10 keV, Δt=10 s light curves. The thresholds, as well as the radius of the source circular extraction regions, were optimized to maximize the signal-to-noise ratio. The background counts were extracted from source-free regions on the same chip. Appropriate response and ancillary files were created using RMFGEN and ARFGEN tasks in the SAS, respectively. Spectra were binned in order to have at least 20 counts in each bin to ensures the applicability of the χ^2 statistics. We restricted the analysis of the PN data in the 0.5 – 10 keV range and the spectral fitting were performed using XSPEC version 11.2 software package (Arnaud 1996). The quoted errors on the model parameters correspond to a 90% confidence level for one interesting parameter ($\Delta\chi^2 = 2.71$).

3 X-RAY SPECTRAL ANALYSIS

The X-ray spectra of Seyfert 2 galaxies can be approximated by a two-component continuum plus an Fe Kα line (e.g., Turner et al. 1997). We apply this model, labeled Model 1, in our fitting procedure, consisting of an absorbed power-law plus a unabsorbed power-law as the soft X-ray component to represent the contribution of scattered emission from the AGN and/or host galaxy. This unabsorbed power-law is either fixed to the value of intrinsic power-law or left free to vary in the spectral fits. Our selection then is based on the comparison of the χ^2 statistics obtained in the best fits. The possible presence of a narrow emission line centered at 6.4 keV originating from neutral iron has also been checked, and modeled with a single Gaussian line. All models discussed in this paper include the Galactic absorption to the line of sight. The unfolded $XMM-Newton$ PN spectra after background subtraction are shown in Figure 1 and compared with model spectra. The best-fit spectral parameters are summarized in Table 2.

3.1 Notes on Individual Sources

NGC 513, MCG -3-58-7, NGC 7682: Model 1 describes the 0.5 – 10 keV spectrum of all three sources well with acceptable reduced χ^2 ($\sim$1). The absorption-corrected 2 – 10 keV luminosities according to the model are 4.9$\times10^{42}$ erg s^{-1} for NGC 513, 3.9$\times10^{42}$ erg s^{-1} for MCG -3-58-7, and 2.05$\times10^{42}$ erg s^{-1} for NGC 7682.

F02581-1136: The $XMM-Newton$ 0.5 – 10 keV spectrum fitted by Model 1 yields an unusual flat hard power-law ($\Gamma = 0.33^{+0.43}_{-1.58}$) with χ^2/dof=29/17. The possibility that the flat photon index is due to the pile-up effect is excluded. On the other hand, there have been two possible spectral models for the observed flat spectrum of Sy2s, the dual absorbed model, and the reflection model. We used the PCFABS model to represent the additional absorbed component with a covering fraction C_f. The dual absorbed model increased Γ to $0.79^{+1.79}_{-1.32}$, with a final χ^2/dof=20/14. We then adopted the unabsorbed pure Compton reflection component from neutral matter (PEXRAV model in XSPEC, e.g., Magdziarz & Zdziarshi 1995). Comparing with the dual absorbed model, such model gives an equally good description of the X-ray spectrum with an associated χ^2/dof=22/15. We measured a $\Gamma = 1.06^{+0.47}_{-1.69}$ and equivalent width (EW) of Fe Kα line of 329^{+338}_{-220} eV. The observed 2 – 10 keV flux is 9.6$\times10^{-13}$ erg s^{-1} cm^{-2}, corresponding to T ratio = 13.7. However, the resulting Fe Kα line EW and T ratio are not expected in pure reflection spectrum. We note that in the dual absorbed model, the photon index is poorly constrained. Taking into account the complexity of spectrum, we finally adopted the dual model to describe the spectrum with hard photon index fixed to 1.8 (χ^2/dof = 21/15), and the main conclusions in this paper will not be affected. The column density of the fully-covering absorber and partially-covering absorber are $7.6^{+8.4}_{-3.6}\times10^{22}$ cm^{-2} and $5.62^{+6.0}_{-2.9}\times10^{23}$ cm^{-2} with a covering fraction of $0.88^{+0.07}_{-0.2}$, respectively. The absorption corrected 2 – 10 keV luminosity associated with this model is 8.4$\times10^{42}$ erg s^{-1}.

NGC 1144: The $XMM-Newton$ image of this object shows a bright nuclear source. The best fits of Model 1 to 0.5 – 10 keV $XMM-Newton$ spectrum yields high intrinsic absorption ($N_{\rm H}$ = 5.62$\times10^{23}$ cm^{-2}). The EW of Fe Kα line at 6.4 keV is 252^{+81}_{-71} eV. The observed 2 – 10 keV flux is 3.14$\times10^{-12}$ erg s^{-1} cm^{-2}, and the intrinsic 2 – 10 keV luminosity is 3.14$\times10^{43}$ erg s^{-1}. Prieto et al. (2002) reported this object as an unobscured one, and 0.2 – 2.4 keV flux of 1.1$\times10^{-13}$ erg s^{-1} cm^{-2}, on the basis of fits to $ROSAT$/PSPC spectrum. We point out that the soft-band X-ray data is not sufficient to estimate the X-ray absorption towards nuclear region (see Fig. 1). The fitted 0.2 – 2.4 keV flux in $XMM-Newton$ spectrum is 1.0$\times10^{-13}$ erg s^{-1} cm^{-2}, consistent with the result of $ROSAT$/PSPC spectrum.

NGC 6890: This source is the weakest Sy2 in the present sample with log L$_{[\rm O\ III]}$ = 40.86 erg s^{-1} (<41 erg s^{-1}). The $XMM-Newton$ observation of this object shows weak nuclear emission. The spectrum is described by a power-law ($\Gamma = 2.54^{+0.47}_{-0.43}$) but without intrinsic absorption. The fitted 2 – 10 keV luminosity is 1.0$\times10^{40}$ erg s^{-1}, consistent with a low luminosity nuclei. The observed 2 – 10 keV flux of 6.9$\times10^{-14}$ erg s^{-1} cm^{-2}, however, gives the T ratio ($\rm F_{2-10\ keV}/F_{[O\ III]}$) of 0.14, suggesting heavy obscuration on nuclear region (Bassani et al. 1999, Guainazzi et al. 2005). Here, we consider it as a Compton-thick one, and give a a lower limit of 10^{24} cm $^{-2}$ to N$_{\rm H}$, though longer exposure observations are crucial to shed light on the nature of absorption in X-rays in this object.

UGC 6100: The $XMM-Newton$ observation of UGC 6100 have been strongly affected by bright background. The poor signal-to-noise prevented us from attempting detailed spectral fits. Here we give only a very rough, approximate description of the 0.5 – 10 keV spectrum in terms of a single power- law with photon index fixed at 1.8. The resulting 2 – 10 keV flux is 5.0$\times10^{-14}$ erg s^{-1} cm^{-2} and T ratio is 0.05 (<0.1), indicating Compton-thick obscuration (Guainazzi et al. 2005). Note that UGC 6100 has the highest [O III] luminosity in the present sample, which is related to strong AGN emission. The observed low X-ray flux and thus small T ratio can only be attributed to heavily nuclear obscuration. We regard it as a Compton-thick one in this paper and give a a lower limit of 10^{24} cm $^{-2}$ to N$_{\rm H}$. The observed 2 – 10 keV luminosity is 1.0$\times10^{41}$ erg s^{-1}.

4 DISCUSSION

We find that all four Seyfert 2 galaxies with PBLs are absorbed with $N_{\rm H} < 10^{24}$ cm^{-2}, while two of three Seyfert 2 galaxies without PBLs have evidence suggesting Compton-thick obscuration. This might

indicates that the central region of these Sy2s is viewed differently and the lack of PBLs can be ascribed to obscuration effects. On the other hand, this obscuration might be a signature for the orientation of dusty torus, shedding some light on the nature of nuclear obscuration matter.

It is instructive to show where these seven Sy2s locate in the plots of [O III] λ5007 luminosity versus nuclear obscuration, comparing with the sample we presented in Paper I. Figure 2 shows the plot of the luminosity of the extinction-corrected [O III] λ5007 emission versus different indicators of nuclear obscuration ($N_{\rm H}$, T ratio, and Fe Kα line EW). All the 42 sources in Paper I and 7 new sources in this paper are plotted. The locus of these targets in the diagram are generally consistent with the results of Paper I that at $\rm L_{[O\ III]} > 10^{41}$ erg s^{-1}, NPBL Sy2s are more obscured than PBL Sy2s. Including these objects (except for NGC 6890), we find the confidence level in the difference of obscuration between luminous PBL and NPBL Sy2s (at $\rm L_{[O\ III]} > 10^{41}$ erg s^{-1}) increases from 92.3% to 96.3% for $N_{\rm H}$, 99.1% to 99.4% for T ratio, and 95.3% to 97.4% for Fe Kα line EW. We also plot in Figure 3 $\rm F_{2-10\ keV}$ vs. $\rm F_{[O\ III]}$ for Compton-thick Sy2s with and without PBLs. The data of UGC 6100 and NGC 6890 located in the diagram follow the correlation for NPBL Sy2s, which have smaller T ratio than those Sy2s with PBLs. The same conclusion can be seen that the smaller T ratio in NPBL Sy2s can be explained by heavier nuclear obscuration and thus higher inclination of torus.

On the other hand, Nicastro et al. (2003) have argued that the driving parameter to the absence of PBLs in Sy2s is the accretion rate (in Eddington units), i. e., PBL Sy2s tend to have Eddington accretion rate above 10^{-3}, while NPBL Sy2s lie at $< 10^{-3}$. Note a contrast argument was made by Zhang & Wang (2006) that NPBL Sy2s tend to have larger accretion rate, like Narrow Line Seyfert 1 galaxies. We carry out a direct comparison with the findings of the above authors. Making use of $L_{\rm X}$ measured by $XMM-Newton$, which is unambiguously related the AGN emission, we estimated the bolometric luminosity of the seven AGNs, assuming a bolometric correction factor of 10 (e.g., Elvis et al. 1994). For two Compton-thick candidates, we applied the correction factor of 60 to estimate the intrinsic X-ray luminosity (Panessa et al. 2006). We obtained published stellar velocity dispersions from Nelson & Whittle (1995), Garcia-Rissmann et al. (2005) and $\sigma_* \sim$ 152, 123, 219, and 156 km s^{-1} for NGC 513, NGC 7682, NGC 1144, and UGC 6100, respectively. For NGC 6890 and F02581-1136, we used $\rm FWHM_{[O\ III]}$ from Whittle (1992), and Heisler et al. (1989), as a proxy for σ_*, σ_*=$\rm FWHM_{[O\ III]}$ /2.35/1.34=78 and 91, respectively (Greene & Ho 2005). From the values of the σ_* and thus the black hole mass, using the $M_{BH}-\sigma_*$ correlation (Tremaine et al. 2002), we are now able to estimate the Eddington ratios L_{bol}/L_{Edd} for the six sources. A comparison with Figure 1 of Nicastro et al. (2003) shows that all six nuclei have Eddington ratios well above the threshold of 1.0×10^{-3} to separate AGNs with PBLs from NPBL sources. The similar large Eddington ratios found for our PBL and NPBL Sy2s are consistent with the findings of Bian & Gu (2007), who suggested that above a given L_{bol}/L_{Edd} threshold of $10^{-1.37}$, PBL and NPBL Sy2s show no difference in their Eddington ratios.

In summary, the $XMM-Newton$ X-ray observations of seven bright Sy2s support the diagram that the absence of PBLs is associated to the higher obscuration level to the nuclear region. The relation between the visibility of PBL and the nuclear obscuration can be understood in the framework of the unified model if the scattering region resides very close to the nucleus and its visibility depends on the viewing angle, as suggested by Heisler et al. (1997). On the other hand, there is no evidence showing that in fairly powerful AGNs ($L_{\rm X} \sim 10^{42}-10^{44}$ erg s^{-1}) the lack of PBLs corresponds to low values of accretion rate onto the central black hole.

Acknowledgements The authors thank L. L. Fan and Z. Y. Zheng for helpful discussions. Support for this work was provided by Chinese NSF through NSF10473009/NSF10533050, and the CAS "Bai Ren" project at University of Science and Technology of China.

References

Alexander, D. M. 2001, MNRAS, 320, L15

Antonucci, R., & Miller, J. S. 1985, ApJ, 297, 621

Antonucci, R. 1993, ARA&A, 31, 473

Arnaud, K. A., 1996, ASP Conf. Series, 101, 17

Bassani, L., Dadina, M., Maiolino, R., Salvati, M., Risaliti, G., della Ceca, R., Matt, G., Zamorani, G. 1999, ApJS, 121, 473
Bian, W., & Gu, Q., 2007, ApJ, 657, 159
Cappi, M., Panessa, F., Bassani, L., et al. 2006, A&A, 446, 459
Cheng, L. P., Zhao, Y. H., & Wei, J. Y. 2002, Chin. J. Astron. Astrophys. (ChJAA), 2, 408
Elvis, M. et al. 1994, ApJS, 95, 1
Garcia-Rissmann, A., et al. 2005, MNRAS, 359, 765
Greene, J. E., & Ho, L. C. 2005, ApJ, 627, 721
Gu, Q., Maiolino, R., & Dultzin-Hacyan, D. 2001, A&A, 366, 765
Gu, Q., & Huang, J. 2002, ApJ, 579, 205
Guainazzi, M., Matt, G., & Perola, G. C. 2005, A&A, 444, 119
Heisler, C. A., Lumsden, S. L., & Bailey, J. A. 1997, Nature, 385, 700
Heisler, C. A., Vader, J. P., & Frogel, J. A., 1989, AJ, 97, 986
Lumsden, S. L., Heisler, C. A., & Bailey, J. A., 2001, MNRAS, 327, 459
Lumsden, S. L., Alexander, D. M., & Hough, J. H., 2004, MNRAS, 348, 1451
Miller, J. S., & Goodrich, R. W., 1990, ApJ, 355, 456
Magdziarz, P., & Zdziarski, A, 1995, MNRAS, 273, 837
Moran, E. C., Barth, A. J., Kay, L. E., Filippenko, A. V. 2000, ApJ, 540, L73
Nelson, C. H., & Whittle, M., 1995, ApJS, 99, 67
Nicastro, F. Martocchia, A. & Matt, G. 2003, ApJ, 589, L13
Panessa, F. et al. 2006, A&A, 455, 173
Prieto, M. A., Pérez Garcia, A. M., & Rodriguez Espinosa, J. M., 2002, MNRAS, 329, 309
Risaliti, G., Maiolino, R., & Salvati, M., 1999, ApJ, 522, 157
Strüder L., et al. 2001, A&A, 365, L18
Shu, X. W., Wang, J. X., Jiang, P., Fan, L. L., Wang, T. G. 2007, ApJ, 657, 167 (Paper I)
Taniguchi, Y., & Anabuki, N. 1999, ApJ, 521, L103
Tran, H. D., 2001, ApJ, 554, L19
Tran, H. D., 2003, ApJ, 583, 632
Tremaine, S., et al. 2002, ApJ, 574, 740
Turner, M. J. L., et al. 2001, A&A, 365, L27
Turner, T. J., George, I. M., Nandra, K., Mushotzky, R. F. 1997, ApJ, 488, 164
Whittle, M., 1992, ApJS, 79, 49
Young, S., Hough, J. H., Efstathiou, A., Wills, B. J., Bailey, J. A., Ward, M. J., Axon, D. J. 1996, MNRAS, 281, 1206
Zhang, E. P., & Wang, J. M. 2006, ApJ, 653, 137

This was prepared with the ChJAA LaTeX macro v1.2.

Table 1 Summary of the $XMM-Newton$ Observations

Name	z	Coordinates (J2000)	Obs. date	PN net exp. (ks)	Sequence	log($L_{[O\ III]}$) erg cm^{-2} s^{-1}	PBL?
NGC 513	0.0195	01 24 26.85 +33 47 58.0	2006 Jan 28	11.2	0301150401	41.14	Y
NGC 1144	0.0289	02 55 12.20 -00 11 00.8	2006 Jan 28	8.3	0312190401	41.87	N
NGC 6890	0.0081	20 18 18.13 -44 48 25.1	2005 Sep 29	1.26	0301151001	40.86	N
NGC 7682	0.0171	23 29 03.93 +03 32 00.0	2005 May 27	7.14	0301150501	41.76	Y
MCG -3-58-7	0.0315	22 49 37.15 -19 16 26.4	2005 May 09	4.03	0301150301	41.93	Y
F02581-1136	0.0299	03 00 30.64 -11 24 56.7	2006 Jan 23	3.79	0301150201	41.16	Y
UGC 6100	0.0295	11 01 34.00 +45 39 14.2	2005 Oct 27	2.4	0301151101	42.28	N

Table 2 Best-fitting Spectral Parameters

Name (1)	$N_{H_{Gal}}$ (2)	N_H (3)	Γ_{HX} (4)	Γ_{SX} (5)	f_s(%) (6)	EW(Fe Kα) (7)	χ^2/dof (8)	F_{HX} (9)	T (10)
NGC 513	5.16	7.2±0.9	1.66±0.17	2.27±0.27	4.14±0.35	156±55	190/228	3.8	23.8
NGC 1144	6.36	$56.2^{+10.2}_{-9.5}$	1.95±0.47	2.69±0.25	0.86±0.08	252^{+81}_{-71}	85/93	3.14	8.0
NGC 6890	3.52	>100	$2.54^{+0.47}_{-0.43}$	...	...	...	8.8/9	0.069	0.14
NGC 7682	5.16	$93^{+73.6}_{-33.6}$	$2.23^{+0.49}_{-0.36}$	=Γ_{HX}	$0.93^{+0.17}_{-0.16}$	465^{+1375}_{-355}	5/11	0.3	0.35
MCG -3-58-7	2.53	$18.4^{+16.2}_{-9.3}$	$1.89^{+1.46}_{-1.08}$	$3.9^{+0.46}_{-0.41}$	$6.2^{+0}_{-1.1}$	46(<342)	21/19	0.75	2.1
F02581-1136*	4.56	$56.2^{+49.6}_{-26.2}$	1.8†	$4.03^{+0.49}_{-0.44}$	$3.9^{+0.6}_{-0.7}$	303^{+270}_{-213}	21/15	0.89	12.7
UGC 6100	1.19	>100	1.8†	...	...	...	12/18	0.05	0.05

Note: Col. (1): galaxy name. Col. (2): Galactic absorption along the line of sight, in units of 10^{20} cm^{-2}. Col. (3) measured absorption column density, in units of 10^{22} cm^{-2}. Col. (4) power-law photon index. Col. (5) photon index of the soft power-law component. Col. (6): scattering fraction of the soft component. Col. (7): Fe Kα line equivalent width in units of eV. Col. (8): chi-squared values and number of degrees of freedom (dof). Col (9): observed 2-10 keV fluxes, in units of 10^{-12} erg s^{-1} cm^{-2}. Col (10) T: the ratio of $F_{2-10\ keV}/F_{[O\ III]}$. † : fixed. *: The X-ray spectrum for this galaxy is fitted by the dual absorbed model (see the text for details).

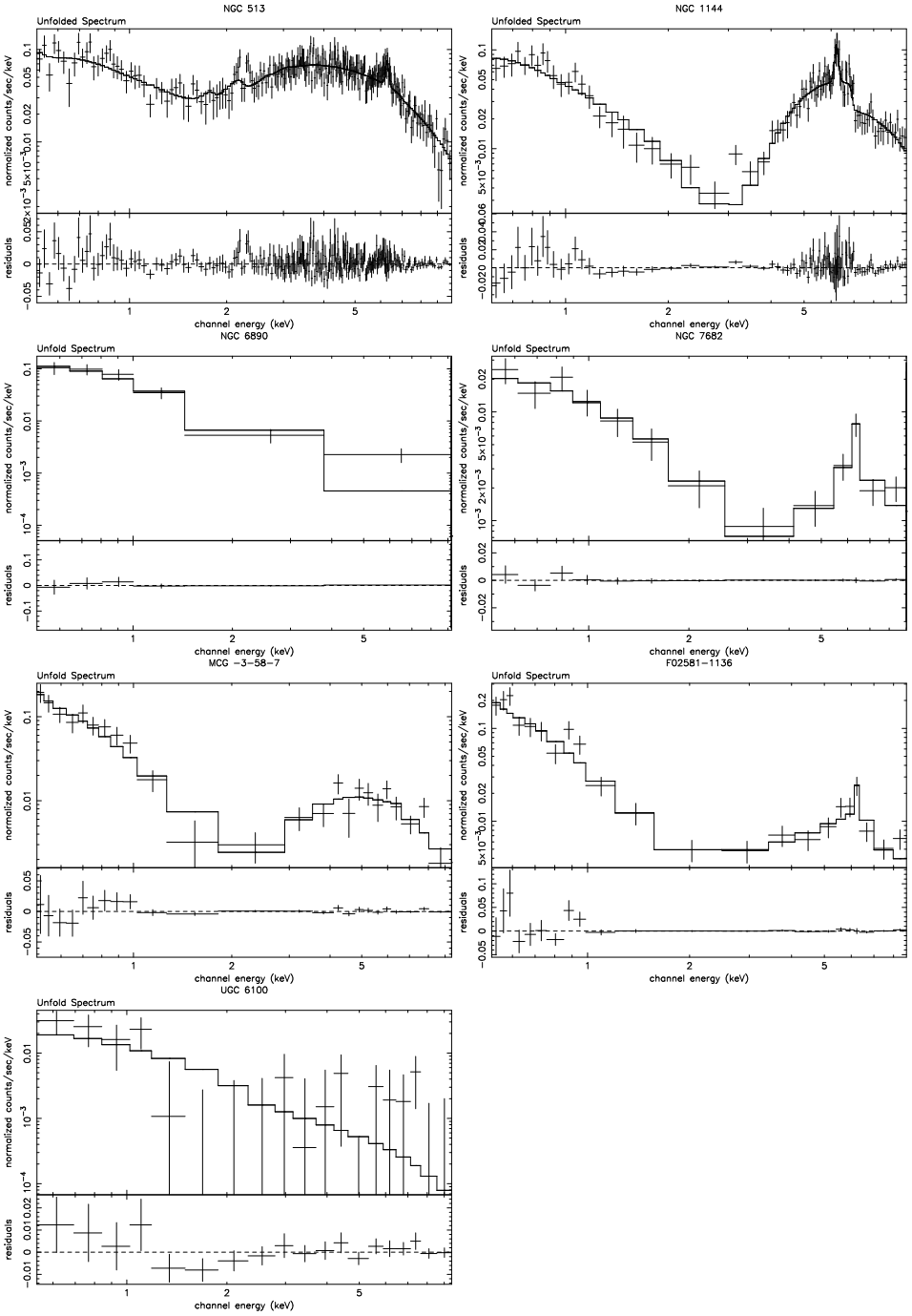

Fig. 1 $XMM-Newton$ PN spectra of seven Seyfert 2 galaxies in our sample. The top panel shows the data and model, and the data/model ratio is shown in the bottom panel.

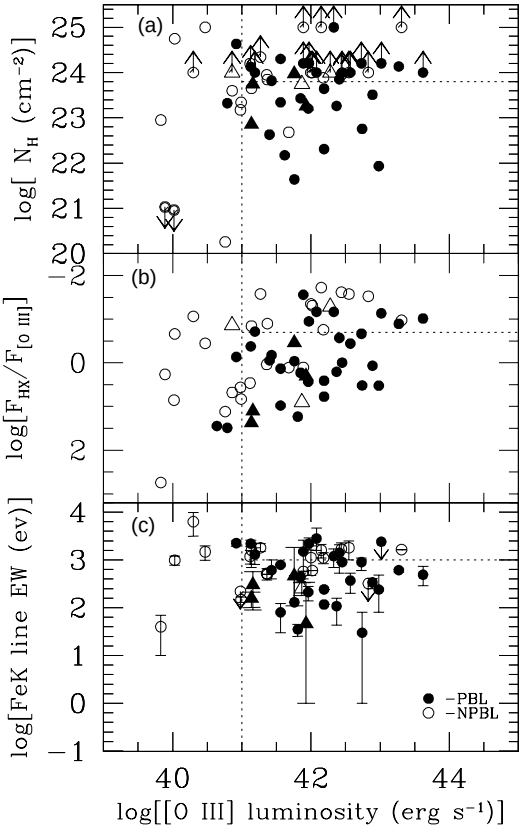

Fig. 2 Plot of [O III] λ5007 luminosity vs. different obscuration indicators for PBL Sy2s (filled symbols) and NPBL Sy2s (open symbols). (a) plots [O III] λ5007 luminosity against $N_{\rm H}$, (b) T ratio, and (c) Fe Kα line EW. The filled circles denote Sy2s in Paper I and the triangles represent objects in present sample.

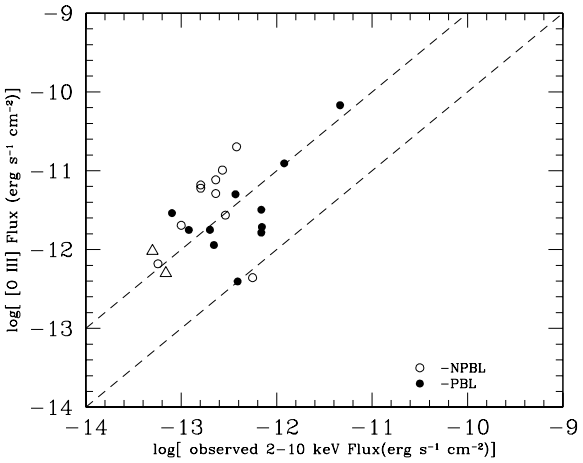

Fig. 3 Observed [O III] flux (extinction-corrected) vs. X-ray (2 – 10 keV) flux for Compton-thick Sy2s (with $N_{\rm H} > 10^{24}$ cm^{-2}). The dashed lines represent $F_{[\rm O\ III]}$ = 10 $F_{2-10\rm keV}$ (upper) and $F_{[\rm O\ III]}$ = $F_{2-10\rm keV}$ (lower). Symbols have the same coding as in Figure 2.